Journal of Statistical Physics, Vol. 76, Nos. 5/6, 1994

Finite-Size Effects for Phase Segregation in a Two-Dimensional Asymmetric Exclusion Model with Two Species

D. P. Foster[1] and C. Godrèche[1]

Received November 4, 1993; final March 8, 1994

We investigate the stationary states of a two-dimensional lattice gas model with exclusion, in the presence of an external field. The lattice is populated by equal numbers of positively and negatively charged particles. An analytical mean-field approach and Monte Carlo simulations give strong evidence of the fact that at any finite density the only relevant stationary state of the system in the thermodynamic limit is inhomogeneous, consisting of a strip of particles transverse to the field. In the inhomogeneous phase, the density profiles and the current measured by Monte Carlo simulations are closely related to those found in mean field. The same is true for the finite-size behavior of the system.

KEY WORDS: Stochastic lattice gas; excluded volume; steady states; phase segregation.

1. INTRODUCTION

Asymmetric exclusion models are simple realizations of driven diffusive lattice gases, which themselves provide simple examples of nonequilibrium systems[1] (see refs. 2 for review). In these models, particles on a lattice hop in a preferred direction with stochastic dynamics and excluded volume interactions.

A number of such models have been studied recently.[3-9] Most of the cases considered are one-dimensional, whether with one or two species of particles and with various types of boundary conditions, often permitting an exact determination of the steady state.

[1] Service de Physique de l'État Condensé, Centre d'Études de Saclay, 91191 Gif-sur-Yvette Cedex, France.

0022-4715/94/0900-1129$07.00/0

We consider here the more difficult situation of a two-dimensional asymmetric exclusion model with two species of particles. Consider a square lattice at 45 deg to the axes, with $N = L_x \times L_y$ sites (Fig. 1) and periodic boundary conditions in both directions. This lattice is populated by equal numbers of particles of two species, which for simplicity we will call positive and negative. These particles are subjected to a uniform field E pointing in the positive x direction. Each site of the lattice is either occupied by *one* particle (positive or negative) or empty. We define two occupation variables: $\tau_M = 1$ if site M is occupied by a positive particle and $\tau_M = 0$ if not. Similarly $\xi_M = 1$ or 0 if site M is occupied by a negative particle or not. The excluded volume condition imposes that only one of the two occupation variables may be nonzero at a time. Hence the occupation variable for holes $1 - \tau_M - \xi_M$ is equal to 1 if site M is empty and to 0 if site M is occupied by one particle of either sign.

The dynamics of the system is defined as follows. During an infinitesimal time interval dt a site M is chosen at random. If it is occupied by a positive particle, this particle hops with probability $a/2$ onto one or the other of the two neighboring sites in the forward direction, and with probability $b/2$ onto one or the other of the two neighboring sites in the backward direction ($a + b = 1$), if the selected neighboring site is empty. If site M is occupied by a negative particle, the same procedure is followed with a and b interchanged. One may relate the probabilities a and b to the field as follows: $a = \exp E/[\exp E + \exp(-E)]$ and $b = \exp(-E)/[\exp E + \exp(-E)]$; hence $a - b = \tanh E$.

This model is, up to a slight geometrical modification, that introduced in ref. 6. Through Monte Carlo simulations, Schmittmann *et al.* observed, for each finite size and when the density of particles is increased, a transition between a homogeneous phase, where all the particles are randomly distributed over the lattice with a uniform density, and an inhomogeneous "blocked" phase, consisting of a strip of particles transverse to the field. The left (right) half of the strip is mainly made of $+(-)$ particles, each half forming a barrier for the other. Hence, in such a phase the current is much lower than in the homogeneous phase; however, it is nonzero for any finite size.

While it is intuitive that such a "blocking" transition should take place for a sufficiently high density, it is unclear how it depends on system size. As pointed out in ref. 6, one may wonder whether this transition survives in the thermodynamic limit.

In this paper we attempt to answer this question. We first consider a mean-field approach to the problem. The equations for the stationary states possess localized solutions, whose analytical expressions are given in the continuum limit. We discuss which solution is selected for given finite

size and density of particles. Finite-size effects enter via a simple scaling function. This permits us to show that, in mean field, the inhomogeneous phase exists down to zero density, in the thermodynamic limit.

Mean-field theory provides a framework for the analysis of the behavior of the real system, given by Monte Carlo simulations. We find that the main characteristics of the mean-field approximation are still present in the real system. In particular its scaling behavior is closely related to that found in mean field. We are finally led to the conclusion that, for any finite density, the stationary state of the system is inhomogeneous in the thermodynamic limit. As a consequence, the transition disappears in this limit.

2. EQUATIONS OF THE MODEL AND MEAN-FIELD APPROXIMATION

The dynamical rules of the model given above allow us to derive equations for the time evolution of the average occupation variables.

Let us consider the occupation of site M by a positive particle. The two sites forward to M are denoted A and B, and the two backward C and D (see Fig. 1). Given a configuration $\mathscr{C}_t$ of the system at time t, characterized by the $2N$ occupation variables $\{\tau_1, ..., \tau_N; \xi_1, ..., \xi_N\}$, the probability of having $\{\tau_M(t+dt)=1\}$ is obtained by summing the probabilities of the following events:

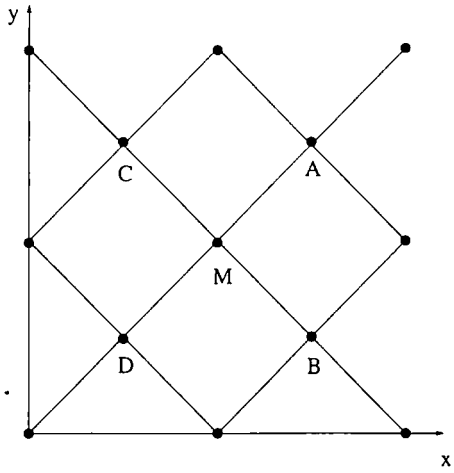

Fig. 1. Geometrical setting of the model. The field E points in the positive x direction.

(i) Neither site M or its neighboring sites are updated; site M is occupied by a positive particle. This occurs with probability

$$\tau_M(t)(1-5dt) \tag{2.1}$$

(ii) Site M is updated; it is occupied by a positive particle; the neighboring sites are occupied. This occurs with probability

$$\tau_M(t)\{[\tau_A(t)+\xi_A(t)+\tau_B(t)+\xi_B(t)]\, a/2 + [\tau_C(t)+\xi_C(t)+\tau_D(t)+\xi_D(t)]\, b/2\}\, dt \tag{2.2}$$

(iii) One of the neighbors of site M is updated; site M is empty; the updated site is occupied by a positive particle which hops onto site M. This occurs with probability

$$[1-\tau_M(t)-\xi_M(t)]\{[\tau_A(t)+\tau_B(t)]\, b/2+[\tau_C(t)+\tau_D(t)]\, a/2\}\, dt \tag{2.3}$$

(iv) One of the neighbors of site M is updated; site M is occupied by a positive particle. This occurs with probability

$$4\tau_M(t)\, dt \tag{2.4}$$

Denoting by $\theta = 1-\tau-\xi$ the occupation variable for holes and averaging on the configurations $\mathscr{C}_t$ leads to

$$d\langle\tau_M\rangle/dt = -\langle a\tau_M(\theta_A+\theta_B)/2 - b(\tau_A+\tau_B)\,\theta_M/2\rangle + \langle a(\tau_C+\tau_D)\,\theta_M/2 - b\tau_M(\theta_C+\theta_D)/2\rangle \tag{2.5}$$

The equation for the evolution of $\langle\xi_M\rangle$ is found in a similar fashion:

$$d\langle\xi_M\rangle/dt = -\langle b\xi_M(\theta_A+\theta_B)/2 - a(\xi_A+\xi_B)\,\theta_M/2\rangle + \langle b(\xi_C+\xi_D)\,\theta_M/2 - a\xi_M(\theta_C+\theta_D)/2\rangle \tag{2.6}$$

These equations indicate that the rates of change of the densities $\langle\tau_M\rangle$ and $\langle\xi_M\rangle$ are given by the difference of currents in and out of site M. Due to the symmetry of the problem, one expects that these currents will not depend on the y coordinate. For instance, $\langle\tau_M\theta_A\rangle$ should be equal to $\langle\tau_M\theta_B\rangle$. However, this symmetry does not reduce the model to a one-dimensional problem, since the time evolution of two-variable correlations depends upon three-variable correlations and so on, which restores the two-dimensional geometry. Therefore the level of complexity of this problem is higher than its corresponding one-dimensional version, whose exact stationary state may be computed by the methods of ref. 4.

Let us then consider a mean-field approximation to these equations. It consists in neglecting correlations between occupation variables. The equations are now only labeled by one (integer) coordinate i along the x direction and the problem is reduced to a one-dimensional problem with size L_x. We will therefore use the language of one-dimensional geometry, though a "site" should be understood as a column of the original two-dimensional lattice.

Setting $p_i = \langle \tau_i \rangle$ (density of positive particles), $m_i = \langle \xi_i \rangle$ (density of negative particles), the evolution equations read

$$\begin{aligned} \frac{dp_i}{dt} &= -(j_i^+ - j_{i-1}^+) \\ \frac{dm_i}{dt} &= -(j_i^- - j_{i-1}^-) \end{aligned} \tag{2.7}$$

where

$$\begin{aligned} j_i^+ &= ap_i(1 - p_{i+1} - m_{i+1}) - bp_{i+1}(1 - p_i - m_i) \\ j_i^- &= bm_i(1 - p_{i+1} - m_{i+1}) - am_{i+1}(1 - p_i - m_i) \end{aligned} \tag{2.8}$$

are the mass currents of positive and negative particles. These equations should be supplemented by the normalization conditions:

$$\sum_{i=1}^{L_x} p_i = \sum_{i=1}^{L_x} m_i = \bar{\rho} L_x \tag{2.9}$$

where $\bar{\rho}$ is the mean density of each species.

Given an initial condition, the system reaches a steady state when $t \to \infty$, for which the left-hand sides of Eqs. (2.7) vanish, implying that the currents (2.8) are conserved. In the following we will investigate the structure of these steady states by studying the solutions of the following discrete nonlinear mapping:

$$\begin{aligned} ap_i(1 - p_{i+1} - m_{i+1}) - bp_{i+1}(1 - p_i - m_i) &= j^+ \\ bm_i(1 - p_{i+1} - m_{i+1}) - am_{i+1}(1 - p_i - m_i) &= j^- \end{aligned} \tag{2.10}$$

These equations have both homogeneous and inhomogeneous solutions, which we will consider in turn.

3. STEADY-STATE SOLUTIONS OF MEAN-FIELD EQUATIONS

3.1. Homogeneous Solutions

A homogeneous phase ($p_i = m_i = \rho$ for all i) is a steady-state solution of the mean-field equations. It is a fixed point both of the temporal equa-

tions (2.7) and of the equations for the steady state (2.10). In this state $\bar{\rho} = \rho$ and the currents for each species are

$$j^+ = -j^- = (a-b)\,\rho(1-2\rho) \tag{3.1}$$

One observes by numerical integration of Eqs. (2.7) that, starting from a slightly perturbed homogeneous phase, this fixed point is stable as long as $\rho \leqslant 1/4$. This observation may be made rigorous by a linear stability analysis of these equations.

Indeed, let us consider a small perturbation to the homogeneous state:

$$\begin{aligned} p_i(t) &= \rho + \varepsilon_i(t) \\ m_i(t) &= \rho + \eta_i(t) \end{aligned} \tag{3.2}$$

Due to the translational invariance of the homogeneous solution, $\varepsilon_i(t)$ and $\eta_i(t)$ should be proportional to the product of a time-dependent amplitude by a plane wave, the wave vector of which is given by $q = 2\pi m/L_x$ (m integer) in order to fulfill periodic boundary conditions. From Eqs. (2.7) one gets

$$\begin{pmatrix} d\varepsilon(t)/dt \\ d\eta(t)/dt \end{pmatrix} = M(q) \begin{pmatrix} \varepsilon(t) \\ \eta(t) \end{pmatrix} \tag{3.3}$$

where $M(q)$ is a matrix whose entries are

$$\begin{aligned} M_{12} &= \rho\{a[\exp(iq) - 1] + b[\exp(-iq) + 1]\} \\ M_{11} &= M_{12} + M_{12}^* \frac{1-2\rho}{\rho} \\ M_{21} &= M_{12}^* \\ M_{22} &= M_{11}^* \end{aligned} \tag{3.4}$$

(asterisk denotes complex conjugation). Its trace and determinant are

$$\begin{aligned} \operatorname{Tr} M &= 2(1-\rho)(\cos q - 1) \\ \det M &= (1-2\rho)[(\cos q - 1)^2 + (1-4\rho)(a-b)^2 \sin^2 q] \end{aligned} \tag{3.5}$$

Finally the eigenvalues of $M(q)$ read

$$\begin{aligned} \Lambda_\pm &= \{\operatorname{Tr} M \pm [(\operatorname{Tr} M)^2 - 4 \det M]^{1/2}\}/2 \\ &= (1-\rho)(\cos q - 1) \pm [\rho^2(1-\cos q)^2 \\ &\quad - (1-2\rho)(1-4\rho)(a-b)^2 \sin^2 q]^{1/2} \end{aligned} \tag{3.6}$$

Since the trace is negative, the real part of the larger eigenvalue can be positive only if the determinant is negative, which occurs when $\rho > 1/4 + \tan^2(q/2)/4(a-b)^2$. The first unstable mode is $q = 2\pi/L_x$. Hence the homogeneous solution is unstable to small perturbations if

$$\rho > \frac{1}{4}\left(1 + \frac{\pi^2}{(a-b)^2 L_x^2}\right) \tag{3.7}$$

This result is given in ref. 6.

3.2. Inhomogeneous Solutions

(i) Given a size L_x and a mean density $\bar{\rho}$, it is easy to obtain inhomogeneous stationary solutions of Eqs. (2.7) by numerical integration. If the mean density $\bar{\rho}$ is not too small, and for an inhomogeneous initial condition, one observes that, e.g., the density profile p_i of the positive particles in the stationary state is the superposition of a localized solution, i.e., a bell-shaped curve around the blocking strip and a background density denoted by ρ. (See, e.g., Fig. 3.)

(ii) It is possible to get a hint of the existence of such localized solutions by a linear stability analysis of Eqs. (2.10) with respect to a perturbation of the homogeneous solution. Setting

$$\begin{aligned} p_i &= \rho + \varepsilon_i \\ m_i &= \rho + \eta_i \end{aligned} \tag{3.8}$$

in Eqs. (2.10) leads to

$$\begin{pmatrix} \varepsilon_{i+1} \\ \eta_{i+1} \end{pmatrix} = M' \begin{pmatrix} \varepsilon_i \\ \eta_i \end{pmatrix} \tag{3.9}$$

where

$$M' = \frac{1}{AB - ab\rho^2} \begin{pmatrix} B^2 - a^2\rho^2 & -(a-b)\rho^2 \\ (a-b)\rho^2 & A^2 - b^2\rho^2 \end{pmatrix} \tag{3.10}$$

with

$$\begin{aligned} A &= a\rho + b(1-2\rho) \\ B &= b\rho + a(1-2\rho) \end{aligned} \tag{3.11}$$

Since M' has a determinant equal to 1, its eigenvalues are

$$\lambda_\pm = \{\mathrm{Tr}\, M' \pm [(\mathrm{Tr}\, M')^2 - 4]^{1/2}\}/2 \tag{3.12}$$

It is convenient to set $\mathrm{Tr}\, M' = 2\cosh\mu$, which yields

$$\lambda_+ = \frac{1}{\lambda_-} = \exp\mu = \frac{1+(a-b)(1-4\rho)^{1/2}}{1-(a-b)(1-4\rho)^{1/2}} \tag{3.13}$$

Defining

$$\tanh E' = (1-4\rho)^{1/2} \tanh E \tag{3.14}$$

one gets $\mu = 2E'$. Hence, when $a-b$ $(=\tanh E)$ is small, $\mu \approx 2E(1-4\rho)^{1/2}$.

Since ε_i and η_i are linear combinations of $(\lambda_+)^i$ and $(\lambda_-)^i$, we can draw the following conclusions. When $\rho \leqslant 1/4$ one has $\lambda_+ > 1$ and $\lambda_- < 1$, i.e., the fixed point $p_i = m_i = \rho$ is hyperbolic: iterating the mapping (2.10) takes the solution exponentially rapidly away from the fixed-point solution. When ρ is larger than 1/4 both eigenvalues are complex with unit modulus, the fixed point is elliptic: the perturbed solution oscillates around the fixed point.

This instability of the homogeneous solution for $\rho \leqslant 1/4$ is the reflection of the presence of an inhomogeneous solution of the mapping (2.10). Starting from the fixed point $p_i = \rho$, p_i is driven away from it exponentially, as long as $\rho \leqslant 1/4$. The drift is governed by λ_+ for the positive i direction and by $\lambda_- = 1/\lambda_+$ for the negative one.

This exponential drift may be simply interpreted as the rise of the profile starting from the background density ρ, which then saturates by nonlinear effects, followed by an exponential decay of the profile, which returns to the fixed point ρ.

As a consequence, the current in the inhomogeneous phase (j^+ in this example) is, up to exponential corrections, given by the same formula as in the homogeneous case, namely $j^+ = (a-b)\,\rho(1-2\rho)$. However, whereas ρ and $\bar{\rho}$ are identical in the homogeneous phase, this is not the case here [see Eq. (4.1) below]. This remark is a key point of the analysis that follows.

The stability analysis of the mapping (2.10) in the space of stationary solutions done here is in no way contradictory with the conclusion of the stability analysis done in Section 3.1 on the temporal mean-field equations (2.7). The same situation occurs in different contexts.[10]

(iii) We now give an analytical description of the density profiles in the continuum limit of Eqs. (2.10). Let us first transform these equations by introducing combinations of p_i and m_i with a given parity. We define

$$\begin{aligned} g_i &= p_i - m_i \\ h_i &= 1 - p_i - m_i \end{aligned} \tag{3.15}$$

where g_i is the charge density and h_i is the hole density, simply related to the local mass density $p_i + m_i$. To these quantities correspond respectively a charge current $j^+ - j^-$ and a mass current $j^+ + j^-$. The latter is zero, by symmetry. (See ref. 6 for similar considerations.) Setting

$$a = \frac{1}{2} + \frac{a-b}{2}; \qquad b = \frac{1}{2} - \frac{a-b}{2} \tag{3.16}$$

we find that the equations for the stationary state read

$$\begin{aligned} &(h_{i+1} - h_i)/2 + (a-b)(g_i h_{i+1} + g_{i+1} h_i)/2 \\ &\quad = j^+ + j^- = 0 \\ &(g_i h_{i+1} - g_{i+1} h_i)/2 + (a-b)[(1-h_i)\, h_{i+1} + (1-h_{i+1})\, h_i]/2 \\ &\quad = j^+ - j^- = 2j^+ \end{aligned} \tag{3.17}$$

where $j^+ = (a-b)\, \rho(1-2\rho)$.

Finding the localized solutions of this discrete mapping is a difficult analytical problem. We therefore consider the continuum limit of these equations. In order to do so we take $a - b \approx E$ small and of the order of the lattice spacing (taken equal to 1 here). In this case p_{i+1} may be approximated by $p(x) + p'(x)$ and any higher-order derivative or any term proportional to the product of $(a-b)$ by a first-order derivative should be neglected. We thus get

$$\begin{aligned} h'/2 + (a-b)\, gh &= 0 \\ (gh' - g'h)/2 + (a-b)(1-h)\, h &= 2(a-b)\, \rho(1-2\rho) \end{aligned} \tag{3.18}$$

where g and h are symmetric functions of x with respect to the origin (primes denote derivatives with respect to the x coordinate). These equations describe an infinite system with boundary conditions $p(\pm\infty) = m(\pm\infty) = \rho$.

Introducing the rescaled variable $2(a-b)\, x$, we find that these equations read

$$\begin{aligned} h' + gh &= 0 \\ gh' - g'h + (1-h)\, h &= 2p(1-2p) \end{aligned} \tag{3.19}$$

Primes denote derivative with respect to the new coordinate. Note that we use the same notations for the profiles after rescaling of the variable. It is now easy to eliminate one of the two functions. Defining

$$w = \frac{1}{h} - \frac{1}{h(\infty)} \tag{3.20}$$

where $h(\infty) = 1 - 2\rho$, one finally gets a single second-order equation

$$w'' = (1 - 4\rho)\, w - 2\rho(1 - 2\rho)\, w^2 \tag{3.21}$$

with $w(\infty) = w'(\infty) = 0$ and $w'(0) = 0$. Integrating once gives

$$\frac{w'^2}{2} = (1 - 4\rho)\frac{w^2}{2} - 2\rho(1 - 2\rho)\frac{w^3}{3} \tag{3.22}$$

which determines

$$w(0) = \frac{3(1 - 4\rho)}{4\rho(1 - 2\rho)} \tag{3.23}$$

Note that Eq. (3.22) does not contain any integration constant, due to the boundary conditions. Setting $\zeta = 2(a - b)(1 - 4\rho)^{1/2}\, x$, we find that Eq. (3.22) leads to

$$\frac{dw}{d\zeta} = \pm w \left(1 - \frac{w}{w(0)}\right)^{1/2} \tag{3.24}$$

The solution of this equation is

$$w(\zeta) = \frac{2w(0)}{1 + \cosh \zeta} \tag{3.25}$$

which is an even function of its argument. We can now derive the relevant profiles:

$$\begin{aligned} h(\zeta) &= \frac{2\rho(1 - 2\rho)(1 + \cosh \zeta)}{3 - 10\rho + 2\rho \cosh \zeta} \\ g(\zeta) &= -\frac{3(1 - 4\rho)^{3/2} \tanh \zeta}{3 - 10\rho + 2\rho \cosh \zeta} \end{aligned} \tag{3.26}$$

from which $p(\zeta)$ and $m(\zeta)$ are easily found:

$$\begin{aligned} p &= (1 - h + g)/2 \\ m &= (1 - h - g)/2 \end{aligned} \tag{3.27}$$

Note that $p(-\zeta) = m(\zeta)$, as expected. Also

$$p(0) = m(0) = \frac{1}{2} - \frac{2\rho(1 - 2\rho)}{3 - 8\rho} \tag{3.28}$$

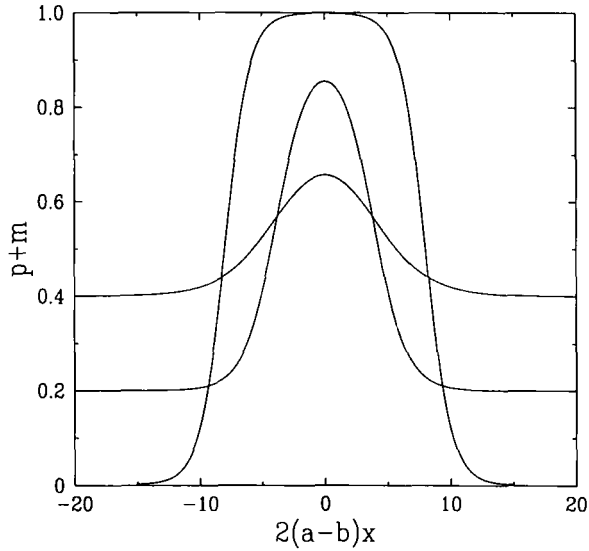

Fig. 2. Analytical continuum mean-field profile $p+m$ for $\rho=0.2$, 0.1, 0.001, plotted against $2(a-b)x$.

As already mentioned, p and m appear as the superposition of a constant background equal to ρ and a localized bump, corresponding to the presence of the blocking strip of particles (Figs. 2 and 3). The area $n(\rho)$ under the bump is easily derived:

$$\begin{aligned} n(\rho) &= \int_{-\infty}^{\infty} [p(x)-\rho]\,dx \\ &= \int_{0}^{\infty} [p(x)+m(x)-2\rho]\,dx \\ &= \int_{0}^{\infty} [h(\infty)-h(x)]\,dx \\ &= [2(a-b)(1-4\rho)^{1/2}]^{-1} \int_{0}^{\infty} [h(\infty)-h(\zeta)]\,d\zeta \end{aligned} \tag{3.29}$$

$n(\rho)$ is the excess number of layers over the background density ρ. When ρ is small it gives a faithful measure of the number of layers of one species in the strip. Noticing that[11]

$$\int_{0}^{\infty} \frac{d\zeta}{\cosh\zeta+\cosh\theta} = \frac{\theta}{\sinh\theta} \tag{3.30}$$

one obtains, with $\cosh\theta = (3-10\rho)/2\rho$,

$$2(a-b)\,n(\rho) = \theta(1-2\rho)(1-8\rho/3)^{-1/2} \tag{3.31}$$

which, in the limit of $\rho \to 0$, gives

$$2(a-b)\,n(\rho) \approx \ln(3/\rho) \tag{3.32}$$

In the vicinity of $\rho = 1/4$ the function $f(\rho) = 2(a-b)\,n(\rho)$ behaves as $3(1-4\rho)^{1/2}$. As a consequence, $n(1/4) = 0$ and $dn(\rho)/d\rho \to -\infty$ for $\rho \to 1/4$.

We end this section by a comparison of the analytical predictions given above with the results obtained from numerical iterations of the discrete mapping (2.10). Since the homogeneous solution is unstable, one has to adjust the initial condition (h_{i_0} and $h_{i_0-1} \approx 1-2\rho$) in order to force the profile h_i to be an even function of the coordinate i. The analytical theory predicts that profiles as functions of $2(a-b)\,x$ or the function $f(\rho)$ should only depend on ρ and not on the field, i.e., $(a-b)$. Figure 3 gives the profiles p, m, and $p+m$ for $\rho = 0.001$, plotted against $2(a-b)\,x$, both for the continuum limit (3.27), and for the discrete case with $a-b = 0.2$. The profiles are practically indistinguishable. This agreement is less good when the field increases. This is clearly shown on Fig. 4, where $f(\rho)$ is plotted

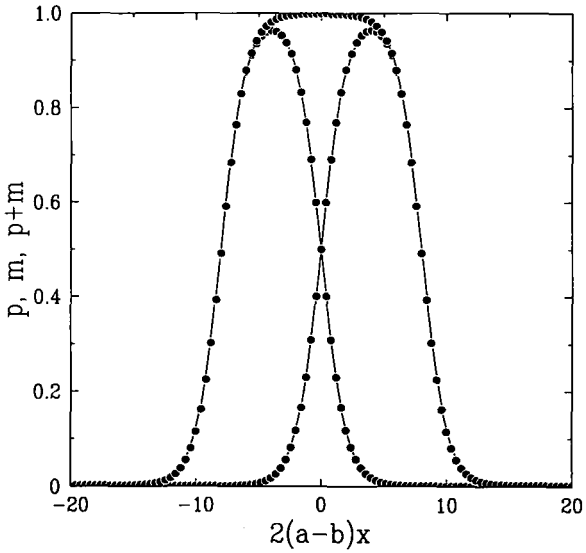

Fig. 3. Mean-field profiles p, m, and $p+m$ for $\rho = 0.001$ plotted against $2(a-b)\,x$ for the continuum limit (continuous line) and for the discrete case (dots) with $a-b = 0.2$ (p on the left, m on the right).

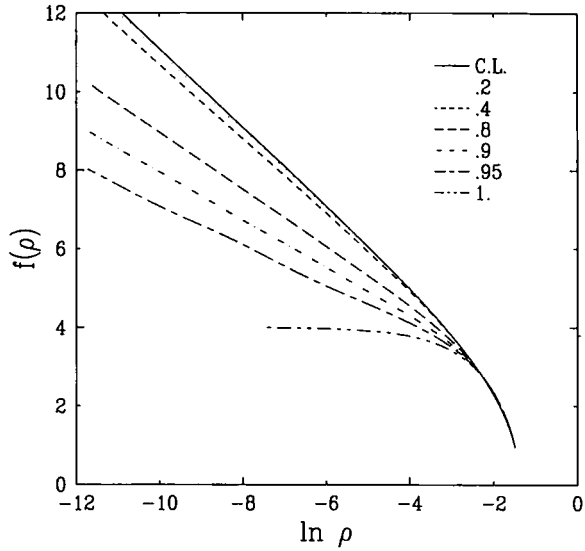

Fig. 4. Plot of $f(\rho)=2(a-b)\,n(\rho)$ against $\ln\rho$ in mean field for the continuum limit (continuous line) and for different values of the field ($a-b=0.2$, 0.4, 0.8, 0.9, 0.95, 1) for the discrete case. $n(\rho)$ is the excess number of layers over the background ρ.

against $\ln\rho$ for the continuum limit (3.31), and for the discrete case with $a-b=0.2$, 0.4, 0.6, 0.8, 0.9, 0.95, 1. The logarithmic behavior of $f(\rho)$ for small ρ is still observed in the latter case.

Remark. It is interesting to compare the results of this section to those given in ref. 6. In this work a phenomenological approach is used in order to derive the continuum mean-field equations. Our equations (3.18) and (3.21) are identical to the equations given in ref. 6 if one identifies their coarse-grained Δ with $2(a-b)$, i.e., with the field. Note that here we parameterize the charge current by the background density ρ, i.e., by the asymptotic behavior of the localized solutions at infinity, whereas in ref. 6 the charge current is fixed by the mean density and by the size of the system. The authors report that they found solutions of these equations in terms of elliptic integrals, which are the solutions of (3.21) for a finite system.

4. FINITE-SIZE EFFECTS AND SCALING IN MEAN FIELD

The previous analysis assumed an infinite size. For any value of the background density ρ there exists a localized solution characterized by its

profiles and by the number of layers in the blocking strip. If the system is finite and the mean density $\bar{\rho}$ given, the question arises of determining which ρ is selected.

From the definition of $n(\rho)$, Eq. (3.29), one has, up to exponential corrections, the following relation between the mean density $\bar{\rho}$, the background density ρ, and the number of layers in the blocking strip:

$$\bar{\rho} = \rho + \frac{n(\rho)}{L_x} \tag{4.1}$$

In this problem finite-size effects only enter through this relation. Equation (4.1) determines which ρ is selected for $\bar{\rho}$ and L_x given. It also gives the combination of observable quantities which should have a simple scaling behaviour, namely

$$\begin{aligned} f(\rho) &= 2(a-b)\, n(\rho) \\ &= 2(a-b)\, L_x(\bar{\rho} - \rho) \end{aligned} \tag{4.2}$$

where ρ is given by $j^+ = (a-b)\,\rho(1-2\rho)$ (hereafter denoted by j). We report the comparison of this prediction with the results obtained by Monte Carlo simulations in Section 5.

The possible solutions of (4.1) appear clearly on a plot of $\bar{\rho}$ as a function of ρ for various values of the product $(a-b)\,L_x$ (Fig. 5, continuum

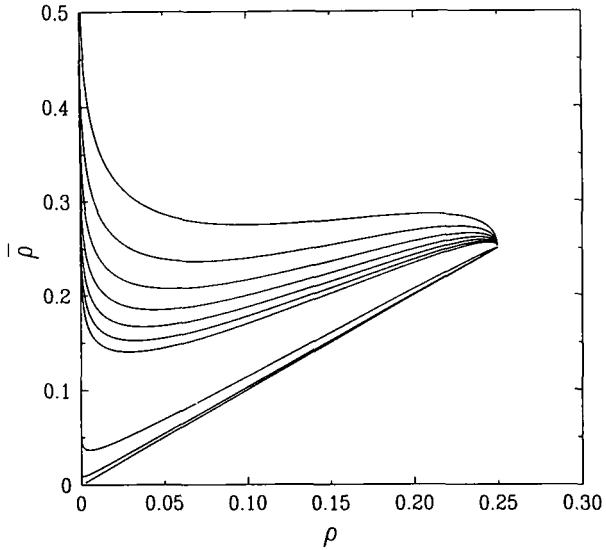

Fig. 5. Plot of $\bar{\rho}$ as a function of ρ in the continuum mean-field theory for $(a-b)\,L_x = 8$, 10, 12, 14, 16, 18, 20, 100, 500 (top to bottom).

mean-field). The homogeneous solution $\bar{\rho} = \rho$ is also plotted on this figure. The discussion hereafter is easily transcribed on a plot of $j/(a-b)$ as a function of $\bar{\rho}$ (Fig. 6). When ρ is small, $\bar{\rho}$ is first a decreasing (logarithmic) function of ρ, along the inhomogeneous curve. It passes through a minimum value $\bar{\rho}_C$, for $\rho = \rho_C$, then increases, reaching the point 1/4 for $\rho = 1/4$ with infinite slope. In the current–density plot this corresponds to a terminal point $C = (\bar{\rho}_C, j_C/(a-b))$ with infinite slope. Approximating $n(\rho)$ by its logarithmic expression (3.32) and computing the derivative of $\bar{\rho}$ with respect to ρ, one gets

$$\rho_C \approx \frac{1}{2(a-b)\, L_x} \tag{4.3}$$

which leads to

$$\bar{\rho}_C \approx \rho_C \ln(L_x/\text{const.}) \tag{4.4}$$

Note the presence of another terminal point D on the right of the plot, where $\bar{\rho}$ is maximum. Again, in the current–density plot this corresponds to a terminal point $D = (\bar{\rho}_D, j_D/(a-b))$ with infinite slope. Using the expansion of $n(\rho)$ in the vicinity of $\rho = 1/4$, one gets

$$\bar{\rho}_D = \frac{1}{4}\left(1 + \frac{9}{(a-b)^2 L_x^2}\right) \tag{4.5}$$

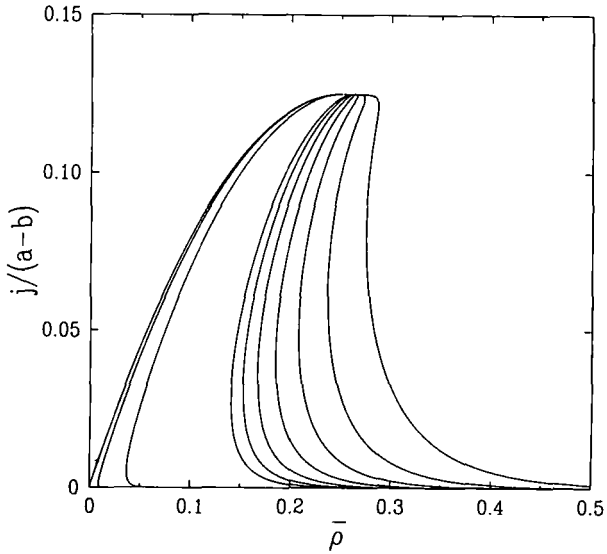

Fig. 6. Same as Fig. 5 for $j/(a-b)$ as a function of $\bar{\rho}$ (right to left).

This expression closely resembles that given in Eq. (3.7), in agreement with the fact that the homogeneous and inhomogeneous solutions should match.

Let us now discuss the possible solutions of Eq. (4.1) for $\bar{\rho}$ and L_x given.

- If $\bar{\rho} < \bar{\rho}_C$, only one value of ρ or j is selected, corresponding to the homogeneous solution.
- If $\bar{\rho} > \bar{\rho}_D$, again only one value of ρ or j is selected, corresponding to the inhomogeneous solution.
- If $\bar{\rho}_C < \bar{\rho} < \bar{\rho}_D$, three possible solutions for ρ or j are selected, two inhomogeneous, one homogeneous. In order to discriminate between them we need to know their stability. The linear stability analysis of the homogeneous solution was done above. We determined the stability of the inhomogeneous solution by numerical means.

Numerical integration of the time-dependent equations (2.7) shows that in the $\bar{\rho}$–ρ plot (or current–density plot) the branch of the inhomogeneous solution with positive slope is never observed. The furthest point reached is the terminal point C. In other terms, if $\bar{\rho}_C < \bar{\rho} < \bar{\rho}_D$, the stationary solution reached is the homogeneous one if one starts with a homogeneous initial condition; it is the inhomogeneous one when starting from an inhomogeneous initial condition.

We have no analytical proof of this instability of the inhomogeneous solution. Note that if such a branch existed, the current would increase with the density in the inhomogeneous phase. We can nevertheless give an interpretation of this instability, when $\rho > \rho_C$, as follows. In the inhomogeneous phase, given L_x and $\bar{\rho}$, the system selects a current, hence a value of ρ ($a-b$ is kept fixed). Suppose $\bar{\rho}$ is decreased, L_x being fixed: ρ increases up to ρ_C. At this point the stable solution becomes the homogeneous one. The inhomogeneous solution appears as a small perturbation of a homogeneous one. One may also look at the same problem from a different angle. Suppose that we now change the size of the system without changing ρ: $n(\rho)$ stays constant and $\bar{\rho}$ decreases, according to (4.1). One is moving on a line $\rho = \text{const.}$ in the $\bar{\rho}, \rho$ plane. So doing, one reaches the terminal point C of the curve corresponding to a size $L = 1/2(a-b)\,\rho$, as given by Eq. (4.3). Again, at this point the stable solution becomes the homogeneous one. L appears as the maximal allowed size for this value of ρ.

In conclusion, according to Eqs. (4.3), (4.4), when the system size L_x goes to infinity, the terminal point $(\bar{\rho}_C, j_C/2(a-b))$ of the stable branch of the inhomogeneous solution goes to zero, whereas the other terminal point $(\bar{\rho}_D, j_D/2(a-b))$ goes to $(1/4, 1/8)$. In other terms, in the limit of an

infinite size, for any density $\bar{\rho} \geqslant 0$ (and less than 1/2), the system possesses an inhomogeneous stationary state. This state is reached if the system is prepared in an inhomogeneous initial condition. We nevertheless inherit of a familiar pathology of the mean-field formalism: since there is no unique stationary state in the thermodynamic limit, the inhomogeneous and homogeneous phases coexist in this limit. It would be interesting to know the relative sizes of the basins of attraction of these two phases, but we made no attempt in this direction.

5. FINITE-SIZE EFFECTS AND SCALING IN MONTE CARLO SIMULATIONS

The method we used for Monte Carlo simulations follows closely the definition of the dynamics given in Section 1. At each step of the simulation, one of the sites of the lattice is chosen at random. If the site is occupied, one of its nearest neighbor sites is chosen according to the following rule. Each of the sites in the preferred direction of the particle (in the direction of the field for the positive particles, and against the field for the negative particles) is chosen with probability $a/2$, while the nearest neighbor sites in the opposite direction are chosen with probability $b/2$

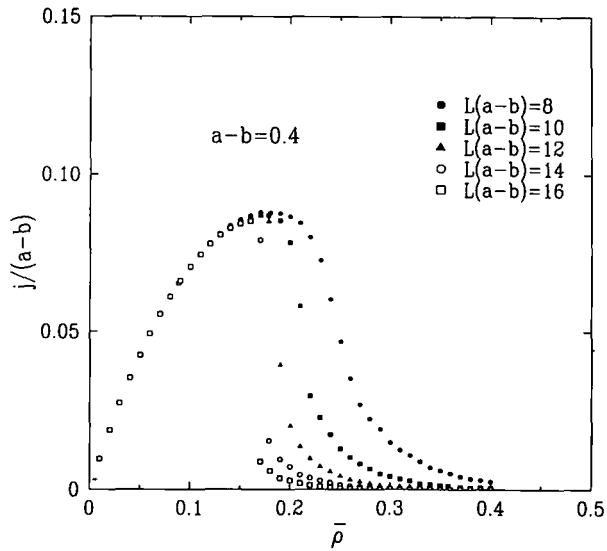

Fig. 7. Plot of $j/(a-b)$ as a function of $\bar{\rho}$ obtained by Monte Carlo simulations for $a-b=0.4$, $L_x=20, 25, 30, 35, 40$ ($L_y=20$).

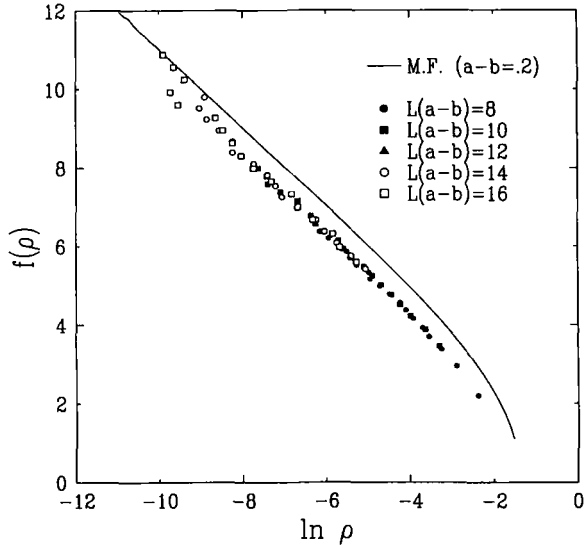

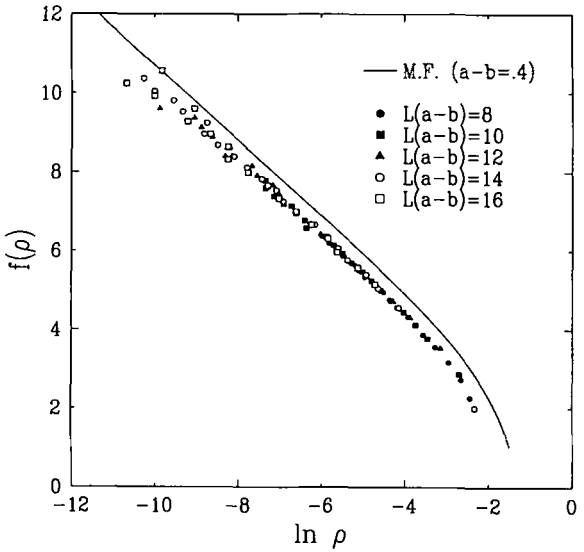

Fig. 8. Plot of $f(\rho) = 2(a-b)\, n(\rho)$ against $\ln \rho$ obtained by Monte Carlo simulations for different values of the field: $a-b = 0.2$, 0.4, 0.8. For each value of the field the corresponding discreet mean-field curve is plotted.

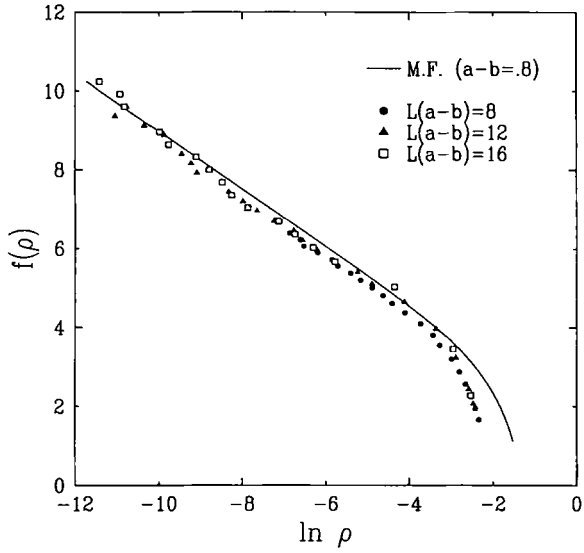

Fig. 8. (*Continued*)

$(a+b=1)$. If the neighbor site selected is empty, the particle is moved from its current site to the chosen site.

We take as time step one Monte Carlo step per site, i.e., the time in which each site has been selected once, on average. At each time step, the current of positive particles is calculated as

$$j^{+}=\frac{1}{L_x L_y}(n_{>}-n_{<}) \tag{5.1}$$

where $n_{>}$ is the number of positive particles which moved with the field, and $n_{<}$ against the field, in the time step. Simulations were run, in general, for 10^5 time steps. Half this time was taken to allow the system to reach the steady state. This was ensured by checking that the current had settled down. Then a measure of the steady-state current was obtained by averaging it over the remaining time. We observed that the results were only weakly dependent on L_y. Simulations were run with $L_y=20$.

Since the dynamics is Markovian and ergodic, it is ensured that the system has a unique stationary state, as long as its size is finite. This was checked by running the simulations from two different initial conditions. The homogeneous one corresponds to placing particles at random on the lattice, the inhomogeneous one to preparing the system in a blocked state. While for generic densities the two initial conditions agreed to a high

precision, metastability effects were noticed close to the transition for the larger lattice sizes, even when performing longer runs of 10^6 time steps. Let us denote by $\bar{\rho}_l$ the terminal point—for L_x fixed—on the inhomogeneous branch of the current–density curve when starting from an inhomogeneous initial condition, and $\bar{\rho}_H$ when starting from a homogeneous one. Metastability is reflected by the fact that $\bar{\rho}_H < \bar{\rho}_l$. These points move to the left when L_x increases. Figure 7 shows the current–density curves obtained when starting from a homogeneous initial condition, for $a - b = 0.4$ and for different sizes. For these sizes, this figure is almost indistinguishable from that obtained when starting from an inhomogeneous initial condition.

In order to check the scaling behavior of the system we plotted the function $f(\rho)$ defined above. Figures 8a–8c show this function for different values of the field: $a - b = 0.2$, 0.4, 0.8, together with the corresponding discrete mean-field one. Since we investigate the behavior of the system in the thermodynamic limit, the scaling region of interest is L large, i.e., small currents. In this region we observe a striking agreement between the logarithmic prediction of mean-field theory and the Monte Carlo data. Note also the increasing agreement between the Monte Carlo curves and the mean-field ones when the field increases.

Thus it appears that finite-size effects obey the same mechanism as in mean field. It is therefore reasonable to assume that the points $\bar{\rho}_H$ and $\bar{\rho}_l$

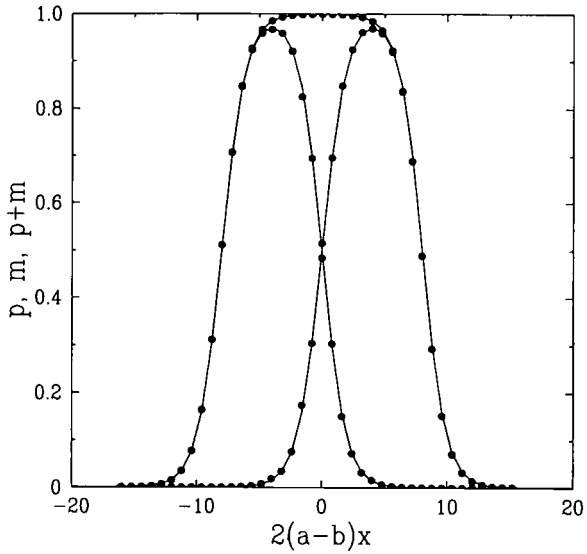

Fig. 9. Density profiles p, m, and $p + m$, obtained by Monte Carlo simulations for $a - b = 0.4$, $L_x = 40$, and $\bar{\rho} = 0.25$ $[f(\rho) \approx 8]$, plotted against $2(a - b)x$. For comparison, the discrete mean-field profiles with $a - b = 0.4$ and $\rho = 0.00078$ $[f(\rho) \approx 8]$ are plotted (continuous line).

are driven to zero when $L \to \infty$. We are thus led to the following conclusion: in the thermodynamic limit, for any finite density $\bar{\rho}$ the only existing phase is inhomogeneous. In the formal limit $\bar{\rho} = 0$, the inhomogeneous phase may coexist with a homogeneous one.

We finally show in Fig. 9 the density profiles in the steady state obtained by Monte Carlo simulations for $a - b = 0.4$, $L_x = 40$, and $\bar{\rho} = 0.25$. These values lead to $j/(a-b) = 0.00043$, hence $f(\rho) \approx 8$. They are in close agreement with the discrete mean-field profiles for the same $f(\rho)$, corresponding to $\rho = 0.00078$. In order to obtain these profiles, we had to overcome the following difficulty. In the steady state any position of the blockage is equally likely. Hence, if the density profile measured from a fixed origin on the lattice is averaged over an infinite time, it is found flat. We solved the problem by choosing a moving origin for the density profile, placed at each time step at the center of mass of all the particles in the system.

6. DISCUSSION AND CONCLUSION

In this paper we aimed to understand the structure of the stationary states of an asymmetric exclusion model with two species. Mean-field theory and Monte Carlo simulations led us to the conclusion that at any finite density the only relevant stationary state is inhomogeneous. As a consequence, the transition observed in ref. 6 disappears in the thermodynamic limit.

The existence of an inhomogeneous phase in the thermodynamic limit is relatively intuitive, as is shown by the following argument. Suppose the system is prepared in a blocked configuration. Then, in the thermodynamic limit, even in the limit of zero density (i.e., with a strip of particles whose thickness increases slowly with the system size), it will take an infinite time for the system to escape such a configuration and reach a homogeneous phase. The analysis done in this paper indicates that a logarithmic increase of the thickness with the size ensures a blockage down to zero density.

In the inhomogeneous phase, there is a good quantitative agreement between the behavior of the real system and that of its mean-field version. This indicates that correlations should be weak in this phase. Indeed it is intuitive that in the blocking strip the moving particles are holes far apart from each other, hence mostly independent, whereas in the outer region the same is true for particles. This agreement should not be so good in the homogeneous phase, since correlations are expected to be stronger. This is actually observed on the currents measured for each finite size. However, by considering a mean-field approximation of the system at the pair level, the currents thus obtained were closer to the currents found in Monte

Carlo simulations. Calculations are unfortunately heavy, so we did not include them here.

There is always a nonzero current in the steady state of the mean-field equations considered here as long as the size is finite. Yet, in the actual one-dimensional model whose mean-field description is given by these equations, the current is zero at any density and for any size L_x. We investigated whether other one-dimensional models for two species with exclusion could lead to segregation effects. In the cases we considered, this effect never appeared. Note that the phenomenon of segregation is a lattice effect which should be present even in higher dimensions, whereas two charged fluids would not block each other.

One would wish to have a better understanding of a number of points on this problem. In particular the stability of the inhomogeneous phase is not done analytically in this paper. We have not tried to measure the sizes of the basins of attraction of the two phases in competition. Neither did we study the possibility of localized steady-state solutions with more than one strip. One would also like to have a general mathematical proof of the disappearance of the transition in the thermodynamic limit. Note that the condition of low fields used to derive analytical mean-field solutions in the continuum limit is not a drawback from a physical point of view. Indeed, if the system already experiences a blockage at low fields it will *a fortiori* do so for higher fields. In the limit of zero field the two species of particles degenerate into a single one. Conversely, the limit of infinite field, or $a = 1$, would be interesting to consider as a starting point for analytical study. Finally, it is worth pointing out the similarity of the questions raised in this work with those analyzed in ref. 12.

ACKNOWLEDGMENTS

It is a pleasure to thank B. Derrida for attracting our attention to this problem, for his continued interest in our work, and for many important discussions. We are particularly indebted to J. M. Luck for enlightening discussions, in particular for a decisive remark on the integrability of the continuum limit of Eqs. (2.10). We have also benefited from interesting comments of S. Aubry and D. Mukamel. D.P.F. would like to acknowledge support from the Royal Society.

REFERENCES

1. S. Katz, J. L. Lebowitz, and H. Spohn, *Phys. Rev. B* **28**:1655 (1983).
2. B. Schmittmann, *Int. J. Mod. Phys. B* **4**:2269 (1990), and references therein; J. Krug and H. Spohn, in *Solids Far From Equilibrium*, C. Godrèche, ed. (Cambridge University Press, Cambridge, 1991), and references therein.

3. B. Derrida, E. Domany, and D. Mukamel, *J. Stat. Phys.* **69**:667 (1992).
4. B. Derrida, M. R. Evans, V. Hakim, and V. Pasquier, *J. Phys. A* **26**:1493 (1993).
5. B. Derrida, S. A. Janowsky, J. L. Lebowitz, and E. R. Speer, *Europhys. Lett.* **22**:651 (1993); *J. Stat. Phys.*, to appear.
6. B. Schmittmann, K. Hwang, and R. K. P. Zia, *Europhys. Lett.* **19**:19 (1992).
7. S. A. Janowsky and J. L. Lebowitz, *Phys. Rev. A* **45**:618 (1992).
8. O. Biham, A. Middleton, and D. Levine, *Phys. Rev.* **46**:R6124 (1992).
9. E. Domany and G. Schütz, *J. Stat. Phys.* **72**:277 (1993).
10. S. Aubry, private communication.
11. I. S. Gradshteyn and I. M. Ryzhik, *Tables of Integrals, Series, and Products*, 6th ed. (Academic Press), 3.514–1, p. 345.
12. M. Aizenman and J. L. Lebowitz, *J. Phys. A* **21**:3801 (1988).